Talanta 89 (2012) 155–161

Contents lists available at SciVerse ScienceDirect

Talanta

journal homepage: www.elsevier.com/locate/talanta

Ultra-high sensitive ammonia chemical sensor based on ZnO nanopencils

G.N. Dar[a,b], Ahmad Umar[a,*], Shabi Abbas Zaidi[a], S. Baskoutas[b,*], S.W. Hwang[a], M. Abaker[a,b], A. Al-Hajry[a], S.A. Al-Sayari[a]

[a] Collaborative Research Centre for Sensors and Electronic Devices (CRCSED), Centre for Advanced Materials and Nano-Engineering (CAMNE), Najran University, P.O. Box 1988, Najran 11001, Saudi Arabia
[b] Department of Materials Science, Patras University, Patras, Greece

ARTICLE INFO

Article history:
Received 31 August 2011
Received in revised form 1 December 2011
Accepted 2 December 2011
Available online 8 December 2011

Keywords:
ZnO nanopencils
Structural and optical properties
Liquid ammonia sensor
I–V technique

ABSTRACT

This paper reports a very simple, reliable and facile methodology to fabricate ultra-high sensitive liquid ammonia chemical sensor using well-crystalline hexagonal-shaped ZnO nanopencils as an efficient electron mediator. A low-temperature facile hydrothermal technique was used to synthesize ZnO nanopencils. The synthesized nanopencils were characterized in detail in terms of their morphological, structural and optical properties which confirmed that the synthesized nanomaterial is well-crystalline, possessing wurtzite hexagonal phase and possess very good optical properties. A very high sensitivity of ~26.58 μA cm^{-2} mM^{-1} and detection limit of ~5 nM with a correlation coefficient (R) of 0.9965 and a response time of less than 10 s were observed for the fabricated liquid ammonia by *I–V* technique. To the best of our knowledge, by comparing the literature, it is confirmed that the fabricated sensor based on ZnO nanopencils exhibits highest sensitivity and lowest detection limit for liquid ammonia. This research opens a way that simply synthesized nanomaterials could be used as efficient electron mediators for the fabrication of efficient liquid ammonia chemical sensors.

1. Introduction

In recent years, numerous intensive reseacrh efforts in the field of nanotechnology has shown great potential. There has been a significant improvement for the synthesis of desired inorganic nanomaterials as reported by vast literature reported so far. Being at the dimension between approximately 1–100 nm, nanomaterial enabled the various useful applications in diverse fields of the scientific areas.

Nowadays, environmental pollution caused by combustion from vehicles, agricultural sector and industrial leakages of toxic chemical and gases at very alarming rate created havoc in the scientific community [1,2]. Among various environmental pollutants, the liquid ammonia (i.e. ammonium hydroxide) is one of the highly toxic chemicals for human being and wildlife produced in fertilizer and chemical factories. The dissolution of this chemical into running and drinking water may cause severe health problems such as skin, throat, lung cancer and permanent blindness. Therefore, early detection and monitoring of leakage of liquid ammonia in the environment is highly desirable for public safety. In this regard, there have been reports for the detection of ammonia (gas and liquid both) in various forms such as electrochemical sensor, optical sensor, chemiresistive sensor, polyaniline and metal oxide based sensors, biomaterials (L-glutamic acid·HCl) based sensors, *I–V* technique based sensor and so on [3–13]. Among various detection techniques, the *I–V* technique is one of the simplest and easy technique for the efficient detection of various hazardous chemicals and environmental pollutants. For this, various nanostructures were used as efficient electron mediators to modify the electrodes for the fabrication of efficient *I–V* technique based chemical sensor [14–18]. Among various nanostructures, metal oxide nanostructures possess excellent properties and hence used for wide applications [5–10,12–16,19–21]. In metal oxides family, the *II–VI* wurtzite hexagonal-shaped ZnO possess special place due to its own properties and wide applications. The various exotic properties of ZnO include its direct and wide band gap (~3.37 eV), high exciton binding energy (60 meV) much larger than other semiconductor materials, biocompatibility, easy and cost effective synthesis, high electron features, optical transparency, non-toxicity and so on [22–26]. Although, ZnO have excellent properties, there are very few reports of this material as ammonia chemical sensor.

In this paper, we report the fabrication of highly sensitive chemical sensor for the efficient detection of liquid ammonia simply by using ZnO nanopencils. For this, a layer of ZnO nanopencils was coated over the active surface of Glassy carbon electrode (GCE) followed by thermal treatment in an oven in order to obtain a uniform and stable layer. Later, the ZnO modified GCE was used to detect

* Corresponding authors.
E-mail addresses: umahmad@nu.edu.sa (A. Umar), bask@upatras.gr (S. Baskoutas).

0039-9140/$ – see front matter © 2011 Elsevier B.V. All rights reserved.
doi:10.1016/j.talanta.2011.12.006

the liquid ammonia by *I–V* technique. Due to well-crystallinity and higher surface area of the synthesized ZnO nanopencils, the fabricated sensor offers ultra-high sensitivity towards the efficient detection of liquid ammonia. In addition to this, the fabricated sensor also exhibited high regression coefficient and very low detection limit, i.e. in the nanomolar range. Furthermore, it was observed that the proposed ammonia sensor is highly reproducible and stable over a long period of time.

2. Experimental detail

2.1. Synthesis of ZnO nanopencils by low-temperature hydrothermal process

Large-quantity synthesis of ZnO nanopencils was done by simple and facile hydrothermal process by using zinc acetate dihydrate ($Zn(CH_3COO)_2{\cdot}2H_2O$) and ammonium hydroxide (NH_4OH) at low-temperature of 125 °C. All the chemicals utilized for the synthesis of ZnO nanopencils were purchased from Sigma–Aldrich and used as received without further purification. In a typical reaction process, 0.05 M zinc acetate was mixed with 0.05 M ammonium hydroxide solution, both made in 50 mL DI water, under contineous stirring. Few drops of ammonium hydroxide were added to maintain the pH of the solution 10.0. The final solution was vigorously stirred for 30 min and consequently transferred to teflon lined autoclave which was then sealed and heated upto 125 °C for 8 h. After terminating the reaction, the autoclave was allowed to cool at room-temperature and the obtained products were washed several times with DI water and ethanol, sequentially and dried at 45 °C. The as-synthesized products were investigated in terms of their morphological, structural and optical properties.

2.2. Characterizations of ZnO nanopencils by low-temperature hydrothermal process

The as-synthesized products were extensively characterized by various analytical techniques. The general and detailed morphologies were examined by using field emission scanning electron microscopy (FESEM; JEOL-JSM-7600F) and transmission electron microscopy (TEM; JEOL-JEM-2100F) equipped with high-resolution TEM (HRTEM). The crystallinity and crystal phases of the synthesized products was examined by using X-ray diffraction (XRD; PANanalytical Xpert Pro.) measured with Cu Kα radiation ($\lambda = 1.54178$ Å) in the range of 20–65°. The chemical composition was examined by using energy dispersive spectroscopy (EDS) and elemental mapping, both attached with FESEM, and Fourier transform infrared (FTIR; Perkin Elmer-FTIR Spectrum-100) spectroscopy in the range of 465–3750 cm^{-1}. The optical properties of the prepared nanomaterial were examined by using UV–visible spectroscopy (Perkin Elmer-UV/VIS-Lambda 950) and Raman-scattering spectroscopy (Perkin Elmer-Raman Station 400 series) at room-temperature.

2.3. Fabrication and characterization of aqueous ammonia chemical sensor by I–V technique

To fabricate the aqueous ammonia chemical sensor, slurry of as-prepared ZnO nanopencils was made with the addition of conducting binders and coated on glassy carbon electrode (GCE, surface area 0.0316 cm^2). Prior to the modification, GCE surface was polished with alumina-water slurry on a polishing cloth, followed by rinsing with distilled water thoroughly. For the electrode surface modification, firstly, an appropriate composition of nanomaterial (ZnO nanopencils) and conducting agent (butyl carbital acetate) were mixed together and ground to obtain a fine powder using a mortal and a pestle. Later, a slurry was produced by dispersing of as prepared powder in a solvent (acetyl acetate). Finally, a certain amount of the slurry was casted on GCE carefully. The modified GC electrode was then dried kept at 60 ± 5 °C for 4–6 h to get a uniform and dry layer over active electrode surface. A simple two electrode system was used to evaluate the sensing performance of ZnO in which the modified electrode was used as working electrode and Pd wire as the counter electrode. An electrometer (Keithley, 6517A, USA) was used as a voltage source for *I–V* measurement. The current response was measured from 2.0 to +5.0 V while the time delaying and response times were 1.0 and 10.0 s, respectively. The concentration and volume of phosphate buffer solution (PBS) were kept constant of 0.1 M and 10.0 mL, respectively. A wide concentration range of ammonium hydroxide (5 mM to 50 nM) was used for all the experiments. The sensitivity of the fabricated aqueous ammonia chemical sensor was estimated from the slope of the current *vs* concentration from the calibration plot divided by the value of active surface area of sensor/electrode.

3. Results and discussion

3.1. Morphological, structural and optical properties of as-synthesized ZnO nanopencils

The morphological, structural and optical properties of as-synthesized ZnO nanopencils were examined by various techniques and discussed in this section. To evaluate the general morphologies, the as-synthesized products were characterized by FESEM and the micrographs are reported in Fig. 1. The FESEM images clearly confirm that the synthesized materials are pointed nanorods which are grown in large quantity. Interestingly, it is seen that the pointed nanorods are assembled in bunches and each bunch has hundreds of nanorods in it. The lengths of the nanorods are in the range of 6 ± 2 μm. Fig. 1(c) and (d) exhibits the typical high-magnification images of as-synthesized pointed nanorods. It is clear from high-resolution images that the nanorods formed pencil like morphology and this is the reason why these nanorods are called "Nanopencils". The nanopencils exhibit very uniform, smooth and clear hexagonal surfaces throughout their length. The characteristic hexagonal surfaces of as-synthesized nanopencils confirm the good crystallinity and wurtzite hexagonal phase for synthesized product. The diameters of the nanopencils at their tips and surfaces are in the range of 45 ± 10 nm and 250 ± 50 nm, respectively (Fig. 1(c) and (d)).

To examine the crystallinity and crystal quality of the as-synthesized ZnO nanopencils, X-ray diffraction technique was used and the pattern is reported in Fig. 2. Several well-defined diffraction reflections are observed which are well matched with the pure wurtzite hexagonal phase. The calculated lattice parameters for the synthesized ZnO nanopencils were $a = 3.249$ Å, $c = 5.205$ Å which are similar to the reported data in Joint Committee on Powder Diffraction Standards (JCPDS), card no. 36-1451. In addition to this, the obtained results are well consistent with the already reported literature [25,26]. No other peak related with any impurity was detected in the observed pattern, upto the detection limit of X-ray diffraction, confirming that the synthesized nanopencils are made of pure ZnO and possess wurtzite hexagonal structure. For detailed structural investigations, the as-synthesized nanopencils were characterized by TEM equipped with HRTEM and the results are presented in Fig. 3. Fig. 3(a) exhibit the low-magnification TEM images, which exhibits the full consistency with the obtained FESEM results in terms of the morphology, shape and size of the nanopencils. To check more elaborately, a high-resolution TEM (HRTEM) was done for as-synthesized nanopencils which clearly exhibits that the lattice fringes are organized in such a proper manner that no dislocation is seen which clearly confirms that the

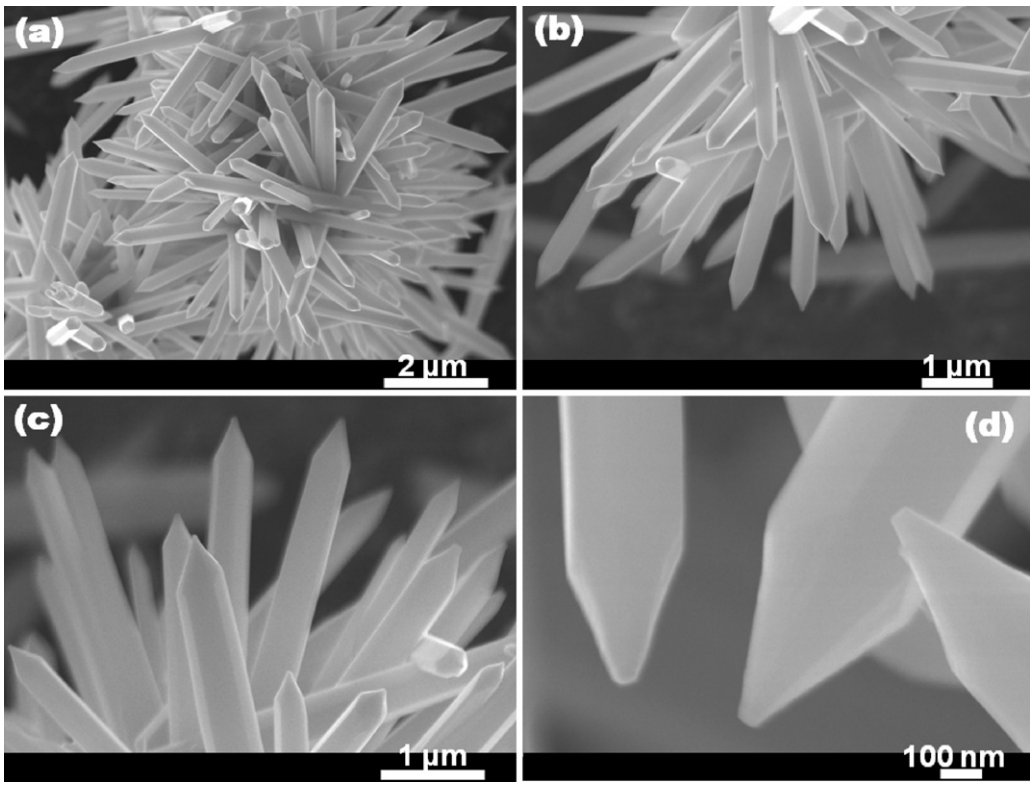

Fig. 1. Low magnification (a and b) and high-resolution (c and d) FESEM micrographs of as-synthesized ZnO nanopencils.

synthesized nanorods are almost defect free and possess good crystallinity (Fig. 3(b)). In addition to this, the distance between two lattice fringes along the longitudinal axis direction, corresponding to the *d*-spacing of ZnO (0 0 0 2) crystal planes, was measured and found to be ~0.52 nm which confirms that the synthesized nanopencils are well-crystalline and having wurtzite hexagonal phase. The inset of Fig. 3(a) exhibits the typical crystallographic growth habit of as-synthesized ZnO nanopencils. It is well known that the shape of any ZnO crystal depends on the relative growth velocities of its different crystal planes [27]. In case of wurtzite hexagonal ZnO, the ideal growth rates in the various crystal facets should be in the order of $[0\,0\,0\,1] > [01\bar{1}\bar{1}] > [0\,1\,\bar{1}\,0] > [0\,1\,\bar{1}\,1] > [0\,0\,0\,\bar{1}]$ under hydrothermal condition [27]. According to the ideal growth rates in various crystal facets, the growth along the [0 0 0 1] direction is maximum and the synthesized nanorods contains $\pm\{0\,0\,0\,1\}$ crystal planes at their top and bottom and enclosed by the six equivalent $\{0\,1\,\bar{1}\,0\}$ crystal facets [28]. It is known that the fastest growing plane generally tends to disappear and leaving behind the slower growing forms with lower surface energy. Hence, the (0 0 0 1) face is not an equilibrium surface and it is bounded by the growth facets of $\{0\,1\,\bar{1}\,1\}$ which has higher Miller indices but lower specific surface energy compared to the (0 0 0 1) facets. As the specific surface free energy of (0 0 0 1) faces are higher than other growth facets, hence after the growth of $\{0\,1\,\bar{1}\,1\}$ facets, the (0 0 0 1) planes are the most likely remaining facets which appear on the ZnO crystals. Interestingly, it is observed that our as-synthesized ZnO nanopencils follow the same growth pattern as reported in the literature for the growth of ideal wurtzite hexagonal ZnO crystals [29,30].

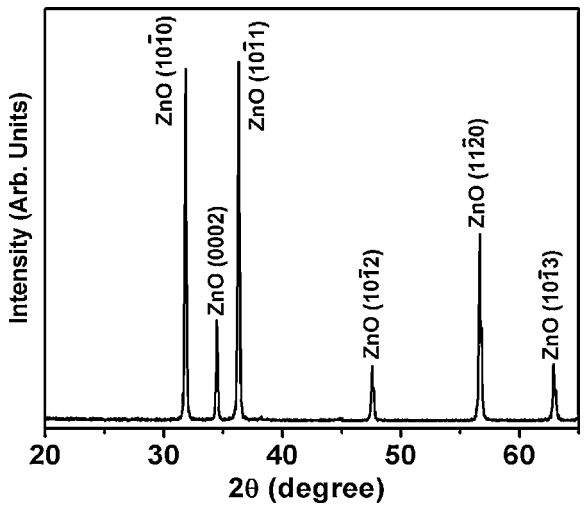

Fig. 2. XRD pattern of as-synthesized ZnO nanopencils.

To check the composition and purity, the as-synthesized ZnO nanopencils were examined by using energy dispersive spectroscopy (EDS) and elemental mapping, both attached with FESEM. Fig. 4(a) exhibits the typical FESEM image of as-synthesized nanopencils and (b) illustrates the typical EDS spectrum of the corresponding nanopencils shown in (a). As can be seen from the obtained FESEM images, the nanopencils are grown in very high density. The corresponding EDS spectrum confirms that the synthesized nanopencils are made of zinc and oxygen. No other impurity peak was observed in the spectrum, up to the detection limit of EDS.

The quality and chemical composition of the as-synthesized ZnO nanopencils were examined by FTIR spectroscopy at room temperature in the range of 465–3750 cm^{-1} and shown in Fig. 5. Several well-defined peaks at 559, 1627 and 3439 cm^{-1} have been observed in the obtained FTIR spectrum. A sharp peak appeared at 559 cm^{-1} is related with metal–oxygen (Zn–O) bond and confirms that the synthesized material is ZnO [31,32]. In addition to the Zn–O band, a very short band appeared at 1627 cm^{-1} and a broad peak at 3439 cm^{-1} was also seen in the spectrum. The appearance

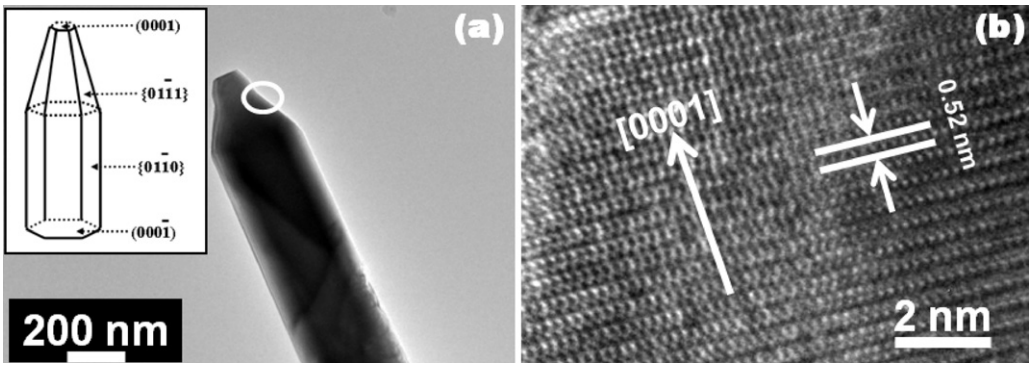

Fig. 3. (a and b) High-resolution TEM micrographs of as-synthesized ZnO nanopencils. Inset of (a) exhibits the schematic of typical crystal habits of as-synthesized ZnO nanopencils by hydrothermal process.

of a very short band at 1627 cm^{-1} is due to the bending vibration of absorbed water and surface hydroxyl, while the broad peak 3439 cm^{-1} is due to the O–H stretching mode [31,32]. In addition to the observed peaks, no other peak related with any functional group was detected in the spectrum which reveals that the synthesized nanopencils are pure ZnO without any significant impurities.

To evaluate the optical properties, the as-synthesized ZnO nanopencils were examined by using a UV–visible (UV–vis) spectrophotometer after dispersion in water by means of ultrasounds at room-temperature. Fig. 6 illustrates the typical UV–vis spectrum of as-synthesized ZnO nanopencils and a well-defined absorption peak at 374 nm is clearly visible. The optical band gap of as-synthesized ZnO nanopencils can be observed by using the Tauc's equation which demonstrates a relationship between absorption

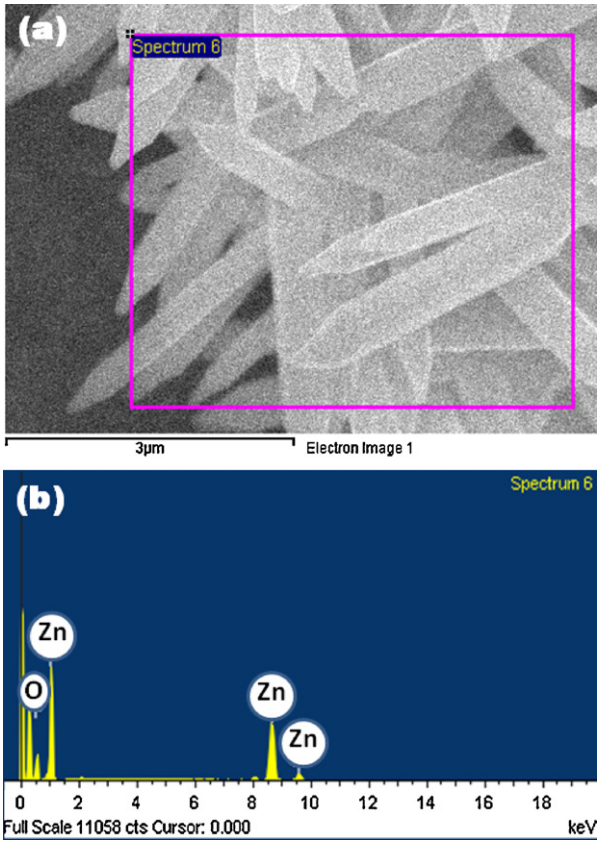

Fig. 4. Typical (a) FESEM image and (b) its corresponding EDS spectrum of as-synthesized ZnO nanopencils.

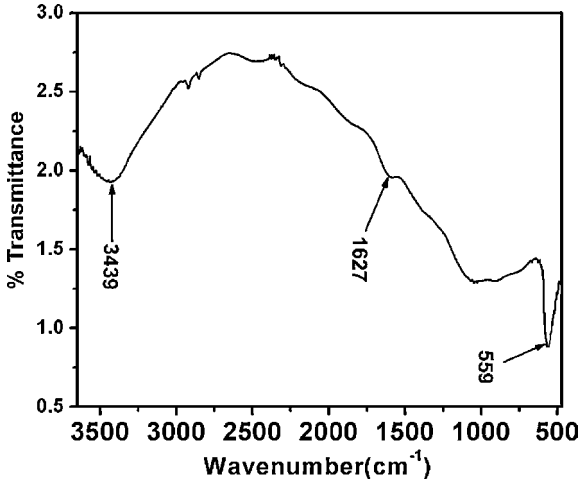

Fig. 5. FTIR spectrum of as-synthesized ZnO nanopencils.

coefficient and the incident photon energy of semiconductors. The Tauc's equation is as follows (Eq. (1)):

$$(ah\nu) = A(h\nu - E_g)^n \quad (1)$$

where α is the absorption coefficient, A is constant, and n is equal to 1/2 for a direct transition semiconductor and 2 for indirect transition semiconductor. According to the equation, the calculated optical band gap for as-synthesized nanopencils was found

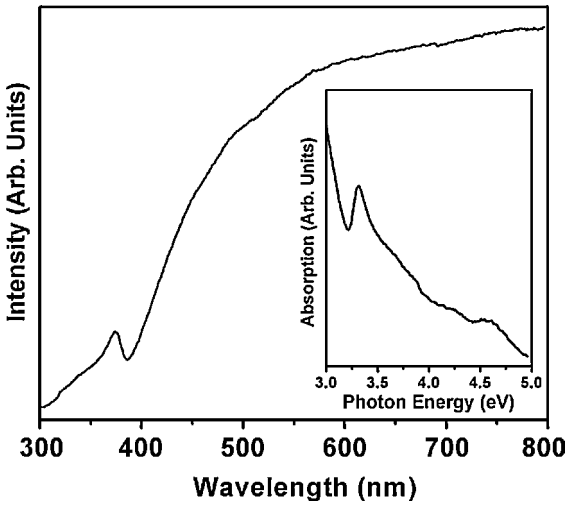

Fig. 6. UV–vis spectrum of as-synthesized ZnO nanopencils.

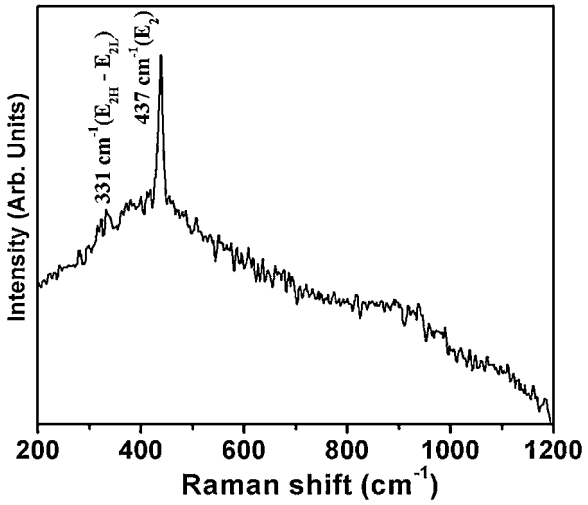

Fig. 7. Raman-scattering spectrum of as-synthesized ZnO nanopencils.

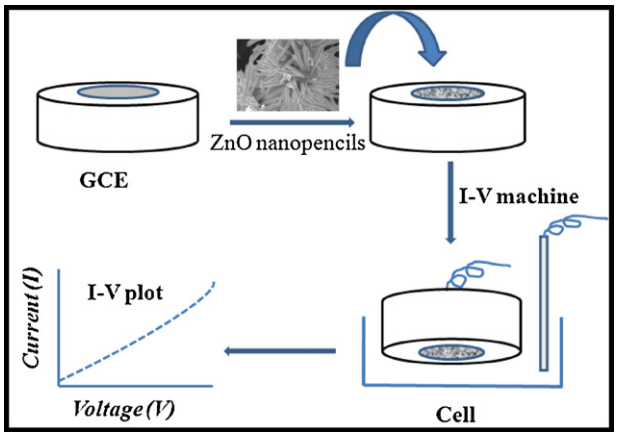

Fig. 8. Schematic representation of ammonia chemical sensor fabrication based on ZnO nanopencils coated GCE electrode and its response by a simple and facile *I–V* technique.

to be ~3.33 eV. The observed optical band gap for the synthesized nanopencils shows fully consistency with the already reported literature [25].

The scattering properties of as-synthesized ZnO nanopencils were characterized by Raman-scattering measurements. ZnO with wurtzite hexagonal crystal structure belongs to C^4_{6V} space group with two formula units per primitive cell. According to the group theory, various Raman active phonon modes exists which are denoted as $\Gamma = A_1 + E_1 + 2E_2$ [33,34]. Among various phonon modes, the A_1 and E_1 modes are polar and split into transverse optical (TO) and longitudinal optical (LO) branches. The E_2 modes are non-polar modes. Fig. 7 shows the typical Raman-scattering spectrum of ZnO nanopencils which exhibits two defined bands, i.e. a sharp and strong band appeared at 437 cm^{-1} and a suppressed and short band at 331 cm^{-1}. The peak appeared at 437 cm^{-1} is attributed to the Raman-active non-polar optical phonon E_2 (high) mode and is a significant band for the wurtzite hexagonal phase of pure ZnO [28]. The other observed short band at 331 cm^{-1} is assigned as E_{2H}–E_{2L} (multi-phonon process) and can be found only when the ZnO is very well crystallized [35]. No other band related with any other optical phonon is seen in the spectrum. Therefore, due to the presence of sharp and strong Raman-active optical phonon E_2 (high) mode and small E_{2H}–E_{2L} mode clearly confirmed that the as-synthesized ZnO nanopencils have good crystal quality with the wurtzite hexagonal phase.

3.2. Ammonia chemical sensor application of as-synthesized ZnO nanopencils

The proposed ZnO nanopencils based chemical sensor was used to detect ammonia in liquid phase which is considered one of the potential hazardous compounds to living beings and wildlife directly or indirectly. The methodology for the detection of ammonia through a typical *I–V* technique has been extensively described in the fabrication part. The schematic representation of sensor fabrication is illustrated in Fig. 8. The ZnO nanopencils based ammonia sensors possess various advantages which include their stability in air and normal environments, biosafety and biocompatibility, high-electrochemical features, non-toxicity, easy fabrication, reliability and many more. Fig. 9 exhibits the typical *I–V* electrical response of the fabricated ammonia chemical sensor based on ZnO nanopencils modified GCE in the absence and presence of 50 nM ammonia in 10.0 mL of PBS solution. It is obvious from the figure that by injecting the target analyte, i.e. ammonium hydroxide, a significant enhancement in current was observed which reflects the high sensitivity of ZnO nanopencils to the analyte. As ZnO possesses good electrocatalytic and fast electron exchange properties, hence it is believed that due to these properties a rapid increase in the current was observed in presence of ammonium hydroxide. In addition to this, the increase in the current could be attributed to the discharge of the trapped electrons into the conduction band. Furthermore, the decomposition of liquid ammonia (Eq. (2)) molecules is an exothermic reaction, releasing the sufficient amount of energy to the electrons to overcome the barrier.

$$NH_4OH_{liquid} \rightarrow NH_4 + OH^- \quad (2)$$

In other words, a catalytic and rate determining reaction occurs on the surface of the ZnO modified electrode. In case of catalytic reaction, the ammonia is first adsorbed on a catalyst, gets split up into ions and then spreads over on the surface and reacts with surface oxygen ions of functional material thereby decreasing the resistance of the sensor and enhancing the current response, because of the ZnO n-type semiconducting behavior.

In general, the detection of any target analyte using metal oxide semiconductors is based upon the oxidation of analyte of interest on sensor surface by the ionized oxygen from the liquid/air interface and subsequent emission of an electron from the ionized species into the conduction band [36]. It has been elucidated in the literature that oxygen plays a vital role in the change of

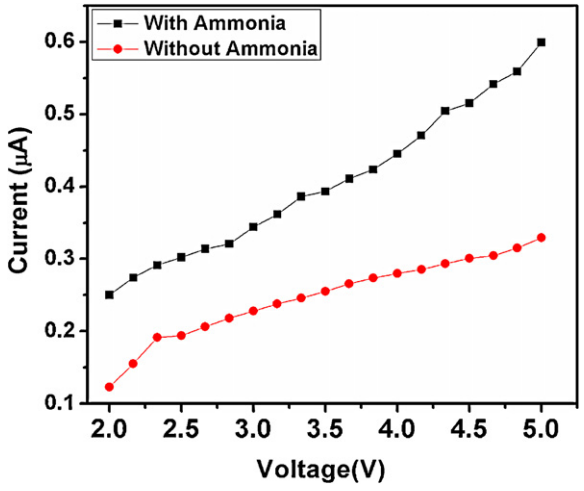

Fig. 9. Typical *I–V* response of glassy carbon electrode (GCE) in 10 mL, 0.1 M PBS solution: (■) with 50 nM ammonia and (●) without the presence of liquid ammonia.

Table 1
Comparison of the performances of the ammonia chemical sensors fabricated based on the utilization of various nanomaterials as electron mediators.

Materials/electrodes	Sensitivity ($\mu A\,cm^{-2}\,mM^{-1}$)	Detection limit	Linear range	References
ZnO nanopencils	~26.5822	~5.0 nM	50 nM to 0.5 mM	Present work
Polyurethane acrylate	8.5254	0.018 μM	0.05 μM to 0.05 M	[11]
β-Fe_2O_3 nanoparticles	0.5305	21.8 μM	77 μM to 0.77 M	[17]
CuO codoped ZnO nanorods	1.549	8.9 μM	–	[19]

electrical behavior of ZnO nanostructures. As shown in Eq. (3), oxygen is adsorbed at nanostructure surface and gets ionized into dynamic oxygen species, such as O^- and O^{2-} by extracting the electron from conduction band of nanostructure surface and hence leading to decrease in the conductance (or increase in resistance).

$$(1/2)O(g) + ne^- \rightarrow O^{n-}ads \quad (3)$$

where O^{n-} ads is adsorbed oxygen ($n = 0, 1, 2$) and e^- is electronic charge.

However, introduction of analyte in the sensor system results into a catalytic reaction described in Eq. (4). The produced ions react with the adsorbed oxygen species and subsequently emit the trapped electrons into the conduction band of nanomaterial. Consequently, this process increases the conductance of nanomaterials and exhibits in the form of electrical signal.

$$A(liquid) \rightarrow B^+ + C^- \quad (4)$$

For further sensor performance investigations, the *I–V* electrical response of the fabricated ammonia chemical sensor based on ZnO nanopencils modified GCE was investigated in various concentrations of ammonium hydroxide in 10.0 mL of PBS solution. For concentration studies, the stock solution of ammonia was prepared by adding the appropriate amount of ammonia in the 0.1 M pH 7.0 buffer. Then, concentrations of ammonia were varied from 5 nM to 5 mM by diluting the stock solution further with the same buffer accurately. Fig. 10(a) exhibits the typical *I–V* response of the fabricated ammonia sensor as a function of ammonium hydroxide concentration at room-temperature. It is observed that the current response increases rapidly with the increase in concentration. Therefore, at lower to higher concentrations of target analyte, the current increases gradually. It can be deduced from current behavior that the number of ions are increased with the increase of the concentration of ammonia corresponding to the rapid electrons transfer relay into conduction band. This results into the enhancement of the sensor response [23,37].

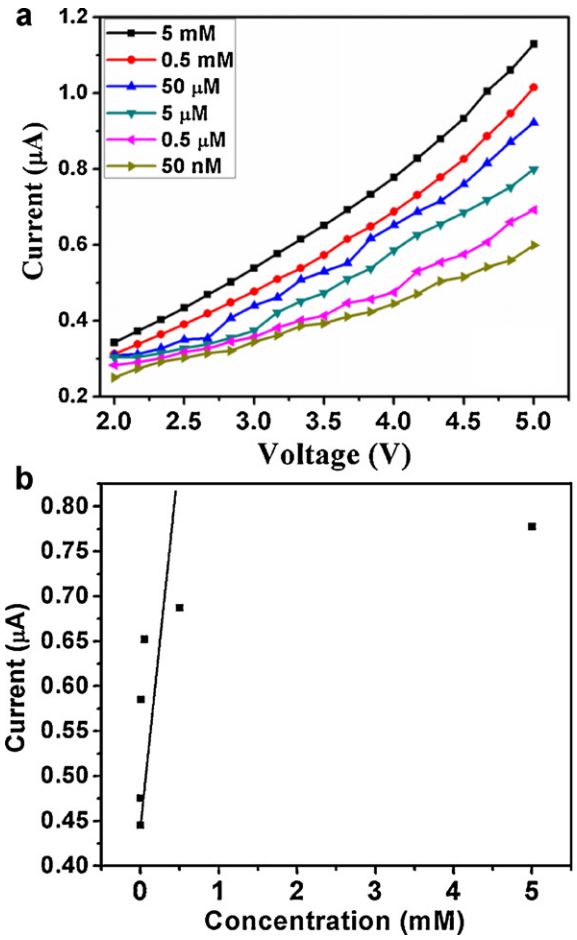

Fig. 10. (a) Typical *I–V* response of ZnO nanopencils modified GCE towards various concentrations (from 50 nM to 5 mM) of liquid ammonia into 0.1 M PBS solution (pH 7) and (b) calibration curve.

The fabricated sensor sensitivity was estimated from the slope of the current vs concentration from the calibration plot shown in Fig. 10(b). The fabricated aqueous ammonia sensor based on ZnO nanopencils exhibits good and reproducible sensitivity of ~26.58 $\mu A/mMcm^2$ and detection limit of ~5 nM with a correlation coefficient (R) of 0.9965 and a short response time (10.0 s). The linear dynamic range was observed to be in the range between 50 nM and 0.5 mM. To the best of our knowledge, the fabricated liquid ammonia chemical sensor exhibits the highest sensitivity ever reported in the literature [11,17,19]. In addition to this, the obtained detection limit of the fabricated sensor is ~5 nM which is lower than the previously reported literature values (Table 1).

The proposed sensor exhibited prominent stability over long period of time. The stability of the present ammonia sensor was determined by measuring the response once a day for 4 weeks. After each measurement, the sensor was stored in a phosphate buffer solution (pH 7.0). No significant decrease in ammonia detection was observed for 3 weeks. After 3 weeks, the response of sensor was gradually reduced due to the weak interaction of ZnO nanopencils electrode and liquid ammonia. This indicates that the fabricated sensor showed not only high but also long term stability. Furthermore, the proposed ammonia sensor showed reproducible behavior too. It is noticeable that the estimated sensitivity of the fabricated sensor is relatively higher than previously reported ammonium hydroxide sensor fabricated based on the utilization of various nanomaterials and/or composite materials modified electrodes [17,19,37]. The observed high-sensitivity and low-detection limit of the fabricated liquid ammonia sensor based on ZnO nanopencils modified electrode was mainly due to the good adsorption ability, rapid catalytic activity and biocompatible nature of as-prepared ZnO nanopencils. A concise Table 1 has been shown to compare the performances of ammonia sensor presented in this study with the already reported values for ammonia sensor fabricated based on the utilization of various electron mediator materials.

4. Conclusion

In summary, a very simple, reliable, reproducible and facile method has been presented to fabricate ultra-high sensitive liquid ammonia chemical sensor. Low-temperature grown,

well-crystalline hexagonal-shaped ZnO nanopencils were used as efficient electron mediators for the fabrication of proposed chemical sensor. The fabricated liquid ammonia chemical sensor exhibits ultra-high sensitivity of $\sim 26.58\,\mu A\,cm^{-2}\,mM^{-1}$ and very detection limit of ~ 5 nM. To the best of our knowledge, the fabricated chemi-sensor exhibits highest sensitivity for liquid ammonia. This research opens a way that simply synthesized nanomaterials could be used as efficient electron mediators for the fabrication of various effective chemical sensors.

Acknowledgements

Authors would like to acknowledge the support of the Ministry of Higher Education, Kingdom of Saudi Arabia for this research through a grant for a Collaborative Research Centre on Sensors and Electronic Devices at Najran University, Saudi Arabia, dated 24/3/1432 H, 27/02/2011. A. Umar and S.A. Al-Sayari are thankful to the Deanship of Scientific Research at Najran University, Saudi Arabia for Grant no. 27/11.

References

[1] A. Sutti, C. Baratto, G. Calestani, C. Dionigi, M. Ferroni, G. Faglia, G. Sberveglieri, Sens. Actuators B 130 (2008) 567–573.
[2] G. Korotcenkov, Sens. Actuators B 107 (2005) 209–232.
[3] B.T. Marquis, J.F. Vetelino, Sens. Actuators B 77 (2001) 100–110.
[4] A.L. Kukla, Y.M. Shirshov, S.A. Piletsky, Sens. Actuators B 37 (1996) 135–140.
[5] G. Ballun, F. Hajdu, G.G. Harsanyi, IEEE 26th Int. Spring Sem. Elect. Tech., vol. 47, 2003, pp. 1–475.
[6] Y.S. Lee, B.S. Joo, N.J. Choi, J.O. Lim, J.S. Huh, D.D. Lee, Sens. Actuators B 93 (2003) 148–152.
[7] S. Christie, E. Scorsone, K. Persaud, F. Kvasnik, Sens. Actuators B 90 (2003) 163–169.
[8] (a) Z. Jin, Y. Su, Y.Y. Duan, Sens. Actuators B 72 (2001) 75–79;
(b) W. Wu, S. Bai, N. Cui, F. Ma, Z. Wei, Y. Qin, E. Xie, Sci. Adv. Mater. 2 (2010) 402–406;
(c) G. Neri, Sci. Adv. Mater. 2 (2010) 3–15.
[9] (a) C.Y. Shen, C.L. Hsu, K.C. Hsu, J.S. Jeng, Jpn. J. Appl. Phys. 44 (2005) 1510–1513;
(b) D. Narducci, Sci. Adv. Mater 3 (2011) 426–435;
(c) R. Chakravarty, C. Periasamy, Sci. Adv. Mater 3 (2011) 276–283;
(d) C. Periasamy, P. Chakrabarti, Sci. Adv. Mater 3 (2011) 73–79.
[10] C.Y. Shen, C.P. Huang, K.C. Hsu, J.S. Jeng, IEEE Int. Ultrason. Ferroelec. Freq. Control, 2004, pp. 546–548.
[11] S.B. Khan, M.M. Rahman, E.S. Jang, K. Akhtar, H. Han, Talanta 84 (2011) 1005–1010.
[12] B. Karunagaran, P. Uthirakumar, S.J. Chung, S. Velumani, E.K. Suh, Mater. Charact. 58 (2007) 680–684.
[13] H. Nanto, T. Minami, S. Takata, J. Appl. Phys. 60 (1986) 482–484.
[14] M.Y. Faizah, A. Fakhru'l-Razi, R.M. Sidek, A.G. Liew Abdullah, Int. J. Eng. Technol. 4 (2007) 106–113.
[15] D. Haridas, K. Sreenivas, V. Gupta, Sens. Actuators B 133 (2008) 270–275.
[16] H.E.L. Hernandez, C.S. Perez, A.G.J. Valenzuela, Opt. A: Pure Appl. Opt. (2010) 10.
[17] M.M. Rahman, A. Jamal, S.M. Faisal, J. Nanopart. Res. (2011), doi:10.1007/s11051-011-0301-7.
[18] S.B. Khan, M. Faisal, M.M. Rahman, A. Jamal, Talanta 85 (2011) 943–949.
[19] M.M. Rahman, A. Jamal, M. Faisal, Appl. Mater. Interfaces 3 (2011) 1346–1351.
[20] M. Faisal, M.M. Rahman, A. Jamal, A. Umar, Mater. Lett. 65 (2011) 1400–1403.
[21] S. Khan, M. Faisal, M.M. Rahman, A. Jamal, Sci. Total Environ. 409 (2011) 2987–2992.
[22] L. Schmidt-Mende, J.L. MacManus-Driscoll, Mater. Today 10 (2007) 40–48.
[23] A. Umar, M.M. Rahman, S.H. Kim, Y.B. Hahn, Chem. Commun. (2008) 166–168.
[24] M.M. Rahman, A. Umar, K. Sawada, Sens. Actuators B 137 (2009) 327–333.
[25] (a) R. Wahab, Y.S. Kim, D.S. Lee, J.M. Seo, H.S. Shin, Sci. Adv. Mater. 2 (2010) 35–42;
(b) D.P. Singh, Sci. Adv. Mater. 2 (2010) 245–272;
(c) H. Zeng, J. Cui, B. Cao, U. Gibson, Y. Bando, D. Golberg, Sci. Adv. Mater. 2 (2010) 336–358.
[26] J. Wu, D. Xue, Sci. Adv. Mater. 3 (2011) 127–149.
[27] R.A. Laudise, A.A. Ballman, J. Phys. Chem. 64 (1960) 688–691.
[28] A. Umar, Y.B. Hahn, Appl. Phys. Lett. 88 (2006) 173120–173122.
[29] (a) A. Umar, Y.B. Hahn, Nanotechnology 17 (2006) 2174;
(b) P.K. Samanta, P.R. Chaudhuri, Sci. Adv. Mater. 3 (2011) 107–112;
(c) A. Khan, S.N. Khan, W.M. Jadwisienczak, Sci. Adv. Mater. 2 (2010) 572–577.
[30] A. Umar, A. Al-Hajry, Y.B. Hahn, D.H. Kim, Electrochim. Acta 54 (2009) 5358–5362.
[31] A. Al-Hajry, A. Umar, Y.B. Hahn, D.H. Kim, Superlatt. Microstruct. 45 (2009) 529–534.
[32] R.A. Nyquist, R.O. Kagel, Infrared Spectra of Inorganic Compounds, Academic Press, Inc., New York, London, 1971, p. 220.
[33] C.A. Arguelo, D.L. Rousseau, S.P.S. Porto, Phys. Rev. 181 (1969) 1351–1363.
[34] J.M. Calleja, M. Cardona, Phys. Rev. B 16 (1977) 3753.
[35] Y.H. Yang, C.X. Wang, B. Wang, Z.Y. Li, J. Chen, D.H. Chen, N.S. Xu, G.W. Yang, J.B. Xu, Appl. Phys. Lett. 87 (2005) 183109.
[36] S.G. Ansari, Z.A. Ansari, H.K. Seo, G.S. Kim, Y.S. Kim, G. Khang, H.S. Shin, Sens. Actuators B 132 (2008) 265–271.
[37] A.O. Dikovska, G.B. Atanasova, N.N. Nedyalkov, P.K. Stefanov, P.A. Atanasov, E.I. Karakoleva, A.T. Andreev, Sens. Actuators B 146 (2010) 331–336.